



HAL
open science

Design of Optimal Extrusion Die for a Range of Different Materials

Nadhir Lebaal, Fabrice Schmidt, Stephan Puissant, Daniel Schlaefli

► **To cite this version:**

Nadhir Lebaal, Fabrice Schmidt, Stephan Puissant, Daniel Schlaefli. Design of Optimal Extrusion Die for a Range of Different Materials. *Polymer Engineering and Science*, 2009, 49 (3), pp.432-440. 10.1002/pen.21298 . hal-01716281

HAL Id: hal-01716281

<https://hal.science/hal-01716281v1>

Submitted on 15 Feb 2019

HAL is a multi-disciplinary open access archive for the deposit and dissemination of scientific research documents, whether they are published or not. The documents may come from teaching and research institutions in France or abroad, or from public or private research centers.

L'archive ouverte pluridisciplinaire **HAL**, est destinée au dépôt et à la diffusion de documents scientifiques de niveau recherche, publiés ou non, émanant des établissements d'enseignement et de recherche français ou étrangers, des laboratoires publics ou privés.

Design of Optimal Extrusion Die for a Range of Different Materials

Nadhir Lebaal,¹ Fabrice Schmidt,² Stephan Puissant,¹ Daniel Schläfli³

¹ Institut Supérieur d'Ingénierie de la Conception (GIP-InSIC), Equipe de Recherche en Mécanique et Plasturgie "ERMeP", 27 rue d'Hellieule, 88100 Saint-Dié-des-Vosges, France

² Ecole des mines d'Albi Carmaux (ENSTIMAC), Centre de Recherche Outillages, Matériaux et Procédés "CROMeP", Campus Jarlard-Route de Teillet 81013 Albi Cedex 9, France

³ Mallefer Extrusion SA Route du bois 37, Ecublens, Switzerland

THE coat-hanger melt distributor is a device commonly used in the wire coating process. Its task is to distribute the melt around the conductor uniformly. It is quite common that materials and flow rates differ from what had been specified during the design procedure. This may lead to bad performance with materials of very different rheological properties from the design material. In this article, we present an optimal design approach to avoid this loss of performances. This approach involves coupling a three-dimensional finite element simulation software with an optimization strategy based on a response surface method. The objective is to determine a coat-hanger melt distributor geometry that ensures a homogeneous exit velocity distribution that will best accommodate for a different range of materials. A coat-hanger melt distributor with a manifold of constant width is designed, and a set of flow distribution measurements is established for two different materials. The results of numerical simulation are then validated by comparison with experimental measurements. The effect of material change is also investigated.

INTRODUCTION

The performance of extrusion dies depends, amongst other things, on the design of the flow channel, the rheological properties of the material, and on the operating conditions used during extrusion [1]. To investigate the effect of the geometrical parameters on the flow distribution in the coat-hanger die, Wang [2] studied the influence of the manifold angle and the contour of the cross section of the flow channel on the exit velocity distribu-

tion using a three-dimensional (3D) finite element code with isothermal flow of power law fluids.

Design of experiment, in particular the Taguchi method [3], allows obtaining valuable information on the important variables of the process. The effects of the various factors are represented on graphs to support the discussion and to lead to the identification of key factors to optimize flow distribution. Within this framework, Chen et al. [1] showed, using Taguchi method, how the operating conditions, the type of materials, and the geometry of the die affect the velocity distribution at the die exit.

The manifold of a coat-hanger die distributor should be optimized for a uniform velocity distribution at the die exit without excessively increasing the pressure drop across the die. However, die complexity, rheological behavior, and performance requirements lead to a high number of numerical tests where the CPU time is often very high for 3D simulations. However, if optimization is attempted without a specific methodology, the solution will most likely not be optimal. Thus, it appears important to define a methodology for an efficient automatic numerical optimization. Within this approach, we can mention Smith et al. [4, 5]. The authors modeled both Newtonian and non-Newtonian isothermal flow in a coat-hanger die using a FE implementation of the generalized Hele-Shaw two-dimensional approximation. An SQP algorithm is used to optimize the die geometry in order to minimize pressure drop subject to exit flow uniformity being within a set tolerance. Sun and Gupta [6] have optimized a flat die to obtain a homogeneous velocities distribution using (BFGS) algorithm. A penalty function was introduced to enforce a limit on the maximum allowable pressure drop in the die. Carneiro et al. [7] used 3D computational routines based on the finite volume method to optimize the flow channel of a specific profile extrusion die. The numerical results obtained are compared with experimental

Correspondence to: N. Lebaal; e-mail: nadhir.lebaal@insic.fr

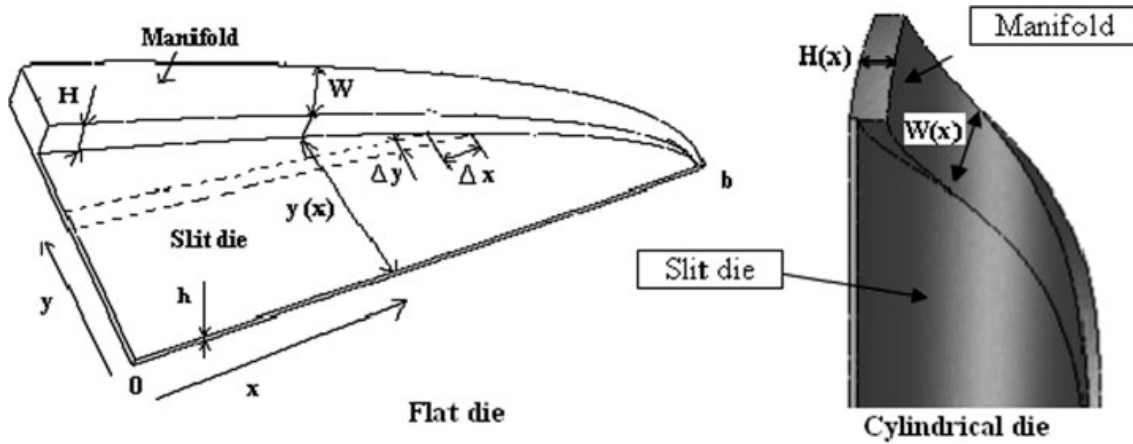


FIG. 1. Sketch of coat-hanger distribution system with wide manifold and narrow slit flow region.

data. The author proposes two optimization algorithms: one based on the SIMPLEX method and a second one that mimics the experimental trial-and-error procedure usually employed in tools manufacture. For the design of profile extrusion die, Michaeli and Kaul [8] used a combination of the finite-element-analysis and flow analysis network to accelerate the iterative optimization process based on the evolution strategy. Reifschneider [9] optimized the manifold angle of the flat die with polynomial RSM using 3D nonisothermal flow analysis. Design variables controlled the manifold angle with the objective to minimize a uniformity index based on local flow rates at a number of predefined sections at the die exit.

More often than not, neither the material nor the extrusion rate corresponds to what had been specified at design time. Because of rheological properties that differ from the design material, the performance may very degrade to an unacceptable level.

Smith [10] shows that exit velocity distribution differs between two materials and that it is influenced by the melt temperature. The author was interested to optimize sheeting die-cavity geometry under multiple operating conditions. To simplify the optimization approach, the lubrication approximation for isothermal flow of power-law fluids is used. Design sensitivities needed for the SQP algorithm are evaluated with the adjoint variable method to improve the performance and accuracy of the computations.

In this article, we present an optimal design approach. This approach involves coupling a 3D finite element simulation software with an optimization procedure (see section "Optimization Procedure"). Our objective is to determine a coat-hanger melt distributor geometry that ensures a homogeneous exit velocity distribution for different materials and multiple operating conditions. The simulation is used to quantify the quality of a die design and includes a nonlinear constraint optimization algorithm to update the die geometry.

The purpose of the experiments described below is to document the effect of material change on the distribution result and to validate the results of numerical simulations

by comparison with experimental data. After the validation, we use the optimization procedure based on a response surface method in order to improve the exit velocities distribution by adjusting geometrical parameters.

EXPERIMENTAL DATA

Die Design

The objective of this study is to find a design procedure for a distribution system that gives uniform exit velocity over the die width. This uniformity should preferably be achieved with a die geometry that is independent of flow rate or polymer viscosity.

Winter and Fritz [11] present a design procedure based on simplified flow model. This model proposes to choose specific cross-sectional geometries for the manifold and calculate the corresponding contour lines $y(x)$ (Fig. 1). The main criteria of the manifold geometry are the invariance to viscosity and flow rate change.

For a manifold of constant width (W) with $W \gg H$, the die design is materials independent. The thickness variation of the manifold is then given by:

$$H(x) = h\sqrt{(b-x)/W}, \quad (1)$$

where $2b$ is the width of distribution system.

The corresponding contour lines $y(x)$ is given as follows:

$$y(x) = 2W\sqrt{(b-x)/W - 1}. \quad (2)$$

To verify the design procedure, one initial distributor was built according to this theory and tested. The distributor has an outer diameter of 106 mm and a slit height of 3 mm, with a flat manifold of constant width (Fig. 2a). The initial manifold height is slightly more than twice the slit height (Fig. 2b). Because of the high aspect ratio, the sidewall effects on the flow are small. Therefore, the flat

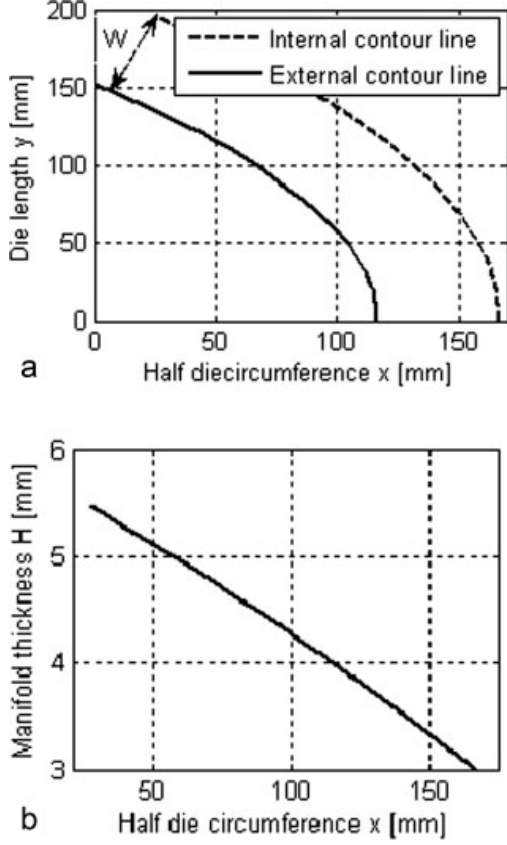


FIG. 2. (a) Manifold contour variation. (b) Manifold thickness distribution.

and wide manifold should result in a long, but material insensitive distributor.

Materials

According to Winter and Fritz [11] and Schläfli [12], the exit velocity distribution of real distributors depends on the slope (power law index) of the viscosity-strain rate

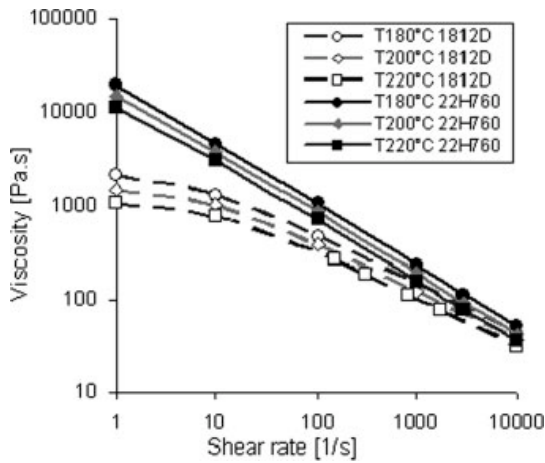


FIG. 3. Viscosity of LDPE (Lupolen 1812D and 22H760) “Carreau & Arrhenius law.”

TABLE 1. Rheological parameters of Lupolen 1812D.

| η_0 (Pa s ^m) | m | τ_s (Pa) | T_{ref} (K) | β (K) |
|-------------------------------|-------|---------------|---------------|-------------|
| 43,434 | 0.347 | 10,555 | 473 | 6156 |

curve. This makes the exit velocity distribution sensitive to the material and flow change. Two different polymers are selected for this example (Fig. 3). A low density polyethylene (LDPE) referred Lupolen 1812D is used because of its rheological behavior. It is noted that the log-log-viscosity curves are linear and the temperature dependence of the viscosity is relatively small.

A second material referenced LDPE 22H760 is selected. It is noted that the width of the transition region between Newtonian and the power-law region is more important.

A Carreau/Arrhenius viscosity model is used to characterize the temperature (T) and shear rate ($\dot{\gamma}$) dependence of viscosity:

$$\eta = \eta_0 \left[1 + \left(\eta_0 \frac{\dot{\gamma}}{\tau_s} \right)^{m-1} \right] \quad (3)$$

with

$$\eta_0(T) = \eta_0(T_{ref}) \exp \left[\beta \left(\frac{1}{T} - \frac{1}{T_{ref}} \right) \right], \quad (4)$$

where η_0 , β , T_{ref} , m , and α are material parameters. The rheological properties of the two polymers (Tables 1 and 2) are obtained from the data bases of Rem3D[®] commercial software (MatDB[®]).

EXPERIMENTAL DATA AND NUMERICAL VALIDATION

Measurements were carried out at Maillefer Extrusion company on a 80 mm, 24 L/D, extruder. In the extrusion head, the extrusion tool for production is replaced by a flow separator setup which divides the flow into eight strips (see Fig. 4). The circumferential melt distribution is obtained by the repeated measurement of the mass flow rate at 36-s intervals for each partial flow. Figure 4 illustrates the diagram of the distributor and the flow separator. The separator is designed to minimize flow resistance, so that it will only marginally influence the distribution. In practice, extrusion tools will have a significant resistance to the flow, which will inherently improve the flow distribution.

By symmetry, the measurements of flow rate on sectors 1 and 5 remain unchanged. On the other hand, for

TABLE 2. Rheological parameters of LDPE 22H 760.

| η_0 (Pa s ^m) | m | τ_s (Pa) | T_{ref} (K) | β (K) |
|-------------------------------|------|---------------|---------------|-------------|
| 1602 | 0.48 | 11,243 | 473 | 4232 |

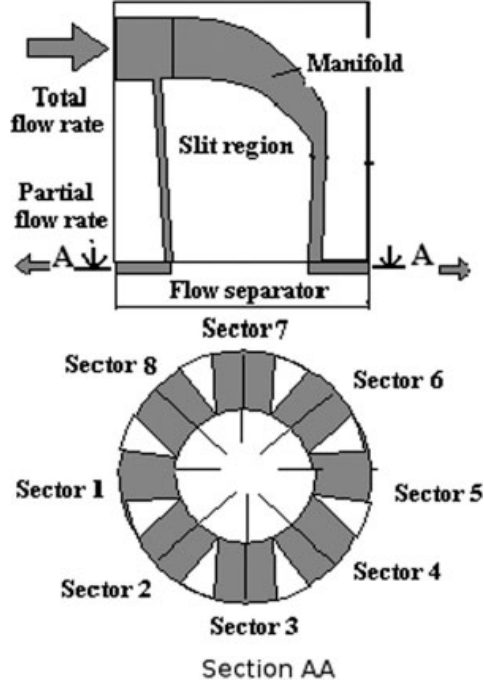


FIG. 4. Principle of flow separator for melt distribution measurement.

sectors 2, 3, and 4, we, respectively, take the average of the measurements of flow established for the sections (2 and 8); (3 and 7); (4 and 6).

The experimental data are obtained for the two different materials mentioned [12]. The results are used to validate the numerical simulation.

The numerical simulations were carried out using Rem3D[®] commercial software [13]. Because of symmetry, we model only half of the die cavity. The finite element model includes 51,512 nodes and 252,593 elements. The process parameters (i.e., flow rate Q_v , die wall temperature T_w , and melt temperature T_m) are listed in Table 3 for the two materials.

For each sector, the dimensionless average velocity \bar{v}^a is defined by

$$\bar{v}_i^a = \left| \frac{\bar{v}_i^s}{\bar{v}} \right| \quad (5)$$

with

$$\bar{v}_i^s = \frac{1}{N^s} \sum_{j=1}^{N^s} v_j^s, \quad (6)$$

where \bar{v} and \bar{v}_i^s are, respectively, the global average velocity and the average velocity for each s section (sector), v_j^s is the velocity in each node j , which belongs to the section S_i , and N^s is the number of nodes for each section on the die exit.

The global relative deviation E_g^s is calculated by the sum of the relative deviations in each section as follows:

$$E_g^s = \sum_{i=1}^{N_s} E_i^s = \sum_{i=1}^{N_s} 100 \cdot |\bar{v}_i^a - 1| \quad (7)$$

TABLE 3. Experimental data.

| Tests | 1 | 2 |
|-------------------------------------|--------------|---------------|
| Materials | PEBD (1812D) | PEBD (22H760) |
| Die wall temperature (T_w) [°C] | 194 | 185 |
| Melt temperature (T_m) [°C] | 193 | 188 |
| Q_1 [kg/h] | 17.87 | 16.77 |
| Q_2 [kg/h] | 18.05 | 16.92 |
| Q_3 [kg/h] | 17.77 | 16.62 |
| Q_4 [kg/h] | 15.84 | 14.85 |
| Q_5 [kg/h] | 12.78 | 12.19 |
| Q_6 [kg/h] | 15.16 | 14.19 |
| Q_7 [kg/h] | 17.1 | 15.78 |
| Q_8 [kg/h] | 17.59 | 16.32 |
| Q_T [kg/h] | 132.16 | 123.64 |
| Q_v [mm ³ /s] | 47,738 | 44,660 |

Figure 5 illustrates the dimensionless average exit velocities distribution as measured and as calculated for each section on the outlet side of the initial die. The manifold of this initial die is of constant width and has an initial aspect ratio of $h/w = 0.11$. According to the theory presented in [11], this design should behave particularly well and be practically material-independent. However, distribution nonuniformity is important and perfectly predicted by the calculation (see Fig. 5). The velocity is more important in the sections (sectors) (1), (2), and (3) and weaker in the sections (4) and (5).

Figure 6 presents the exit velocity distributions, pressures, and shear rate field in the initial geometry. The velocity distributions obtained by 3D finite element model and experimental measurements show the limitations of a design method using a one-dimensional model such as presented by Winter and Fritz [11]. The flow paths between the inner and outer manifold wall become significantly different, and the manifold flow can no longer be treated as a 1D duct flow. The local flow properties across the manifold are no longer constant. This is illustrated by the shear rate field (Fig. 6c), which shows two zones of different shear with a possibility of a stagnating zone with high viscosity and low shear rate close to the rear manifold wall.

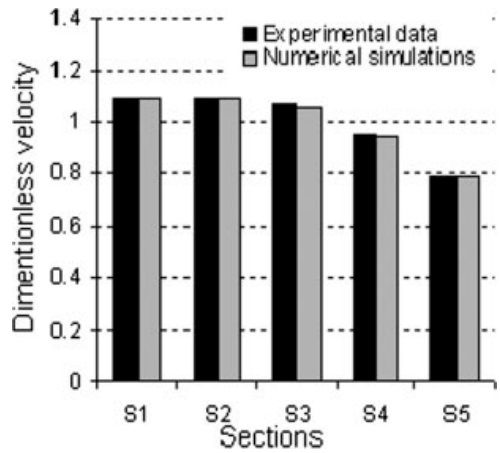


FIG. 5. Calculated and measured velocity distribution (Lupolen 1812D).

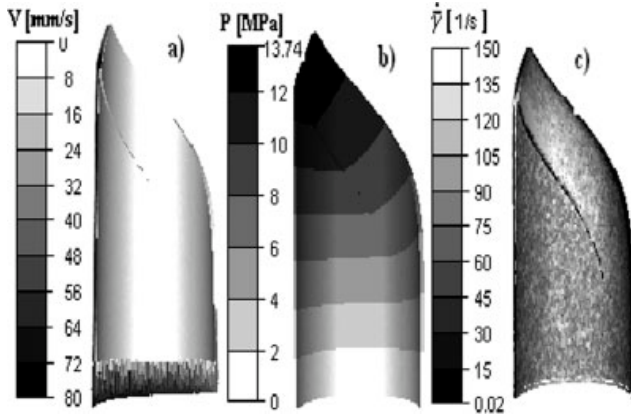


FIG. 6. Simulation results using Rem3D[®] (LDPE Lupolen 1812D). (a) Velocity distributions, (b) pressures, and (c) shear rate field.

The same phenomenon is observed in Fig. 7. The polymer used for this example is LDPE 22H760 with a flow of 124 kg/h. This figure illustrates the calculated and measured exit velocity distribution. We note with this study that the material has a weak influence on the exit velocity distribution as expected from the design theory.

However, the observed nonuniform velocity distribution and the shear rate field (Figs. 6–8) are not predicted by the theory [11]. This is due to the already mentioned 3D character of the manifold flow. Clearly, 3D effects are important for such designs as [11], and they were not taken into account by this theory.

FORMULATION OF THE OPTIMIZATION PROBLEM

Objective and Constraint Functions

The optimization problem and solution procedure described below permit to develop a coat-hanger melt distributor capable of performing well under a range of different materials and various operating conditions.

This optimization problem consists in determining a geometry that results in a homogeneous exit velocity distribution: this corresponds to the minimum of the velocity dispersion (E). The objective has to be reached under the condition that pressure consumption is same or less than the initial distributor; this condition translates into a constraint function (g).

$$\begin{cases} \min J(\Phi) = \frac{E}{E_0} \\ \text{such that } g = \frac{P - (P_0)}{(P_0)} \leq 0 \end{cases}, \quad (8)$$

where (J) is the normalized objective function. The velocity dispersion (E) is defined as:

$$E = \frac{1}{N} \sum_{i=1}^N \left(\frac{|v_i - \bar{v}|}{\bar{v}} \right). \quad (9)$$

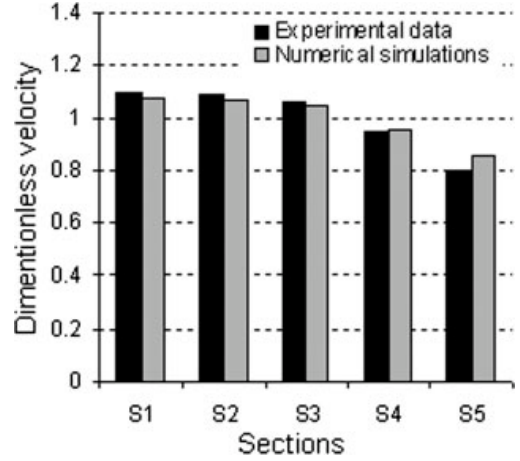


FIG. 7. Calculated and measured velocity distribution (LDPE 22H760).

Variables E_0 and P_0 are, respectively, the velocity dispersion and the pressure in the initial die, N is the total number of nodes at the die exit in the middle plane, v_i is the velocity at exit node i , and \bar{v} is the average exit velocity:

$$\bar{v} = \frac{1}{N} \sum_{i=1}^N v_i. \quad (10)$$

The constraint function (g) is selected in a way to be negative if the pressure is lower than the pressure obtained by the initial die design (the pressure must be even lower compared with the initial pressure).

Design Variables

For a diameter of 106 mm ($b = 166.5$), a slit height of 3 mm and an initial manifold of constant width, the contour lines $y(x)$ and the thickness variation of the manifold are calculated starting from Eqs. 3,4 given by Winter and Fritz [11].

During the optimization procedure, external contour lines of the die (determined by the initial parameters) remain constant. Consequently, two variables will be optimized in order to ensure better exit velocity distribution: manifold thickness and manifold width variation (Fig. 9).

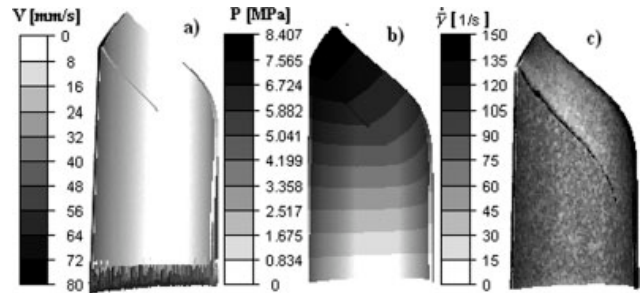


FIG. 8. Simulation results using Rem3D[®] (LDPE 22H760). (a) Velocity distributions, (b) pressures, and (c) shear rate field.

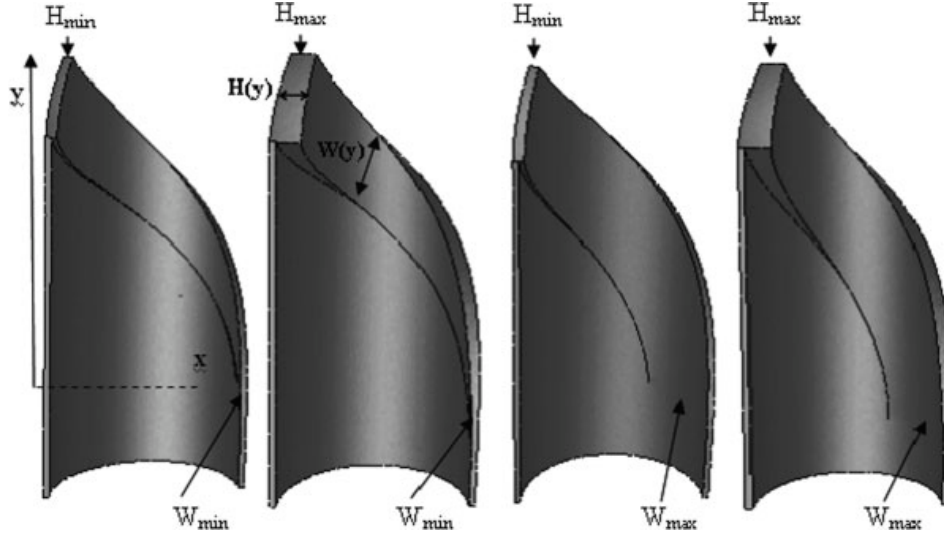


FIG. 9. Optimization variables $W(y)$ and $H(y)$.

Initially, the manifold width W_0 is constant. During the optimization procedure W varies linearly along the length of the manifold (y).

$$W(y) = \hat{P}(y)a, \quad (11)$$

where $\hat{P} = [1 \ y]$ is the polynomial basis function, and $a = \begin{Bmatrix} a_1 \\ a_0 \end{Bmatrix}$ are the unknown coefficients that are determined by the boundary conditions:

$$\begin{cases} W(y_{\max}) = W_0 \\ W(0) = W^k \end{cases} \quad (12)$$

where $W_0 = 50$ mm is the initial manifold width in the entry of the die, and W^k is the manifold width on the outlet side of the die. This parameter can vary during the optimization procedure. The second variable (manifold thickness) varies linearly along the length of the die with:

$$\begin{cases} H(y_{\max}) = H^k \\ H(0) = h \end{cases} \quad (13)$$

where $h = 3$ mm is the slit height of the die and H^k is the manifold thickness at the entrance. This second variable can vary during the optimization procedure. Each variable has its geometrical limitations which are respectively: $5 \leq W^k \leq 60$ mm, $5 \leq H^k \leq 15$ mm (Fig. 9).

To automate the optimization procedure and to save time, a subroutine allowing to treat the CAD and to change the die geometry automatically has been developed in a Matlab[®] environment. From the one-dimensional model [11], we obtain the manifold contour line, and then with the optimization variables, we obtain the manifold thickness and width variations. From the manifold contour line, width, and thickness, a 3D mesh of the coat-hanger melt distributor is generated.

Optimization Procedure

The quality functions (Eq. 8) are implicit compared with the optimization parameters and their evaluations need a complete numerical analysis of the extrusion process. This requires large computation times. To obtain the optimum parameters at low cost and with good accuracy, the Response Surface Method (RSM) is adopted [14, 15] and coupled with an auto adaptive strategy of the research space (Fig. 10). The RSM consists in the construction of an approximate expression of objective and constraint functions starting from a limited number of evaluations of the real function (numerical analysis). To obtain a good approximation, we used a Kriging interpolation [16, 17] technique. In this method, the approximation is computed by using the evaluation points by composite design of experiments.

Once the approximation of the objective and constraint functions are built for each iteration, the Sequential Quadratic Programming (SQP) algorithm is used to calculate the optimal approximate solution which respects the imposed nonlinear constraints. To avoid being trapped in a local optimum, and in order to respect the imposed nonlinear constraint, we use an automatic procedure which launches the SQP algorithm from each point (NP) of our experimental design (Fig. 10a). We choose then the best approximate solution among the NP solutions obtained by the various optimizations. After that, successive local approximations are built in the vicinity of the best approximate solution using a weight function of Gaussian type. The iterative procedure stops when the successive optima of the approximate functions are superposed with a tolerance $\varepsilon = 10^{-6}$ (Test no. 1). Finally, a last evaluation is carried out to obtain the real response in the optimization iteration.

An adaptive strategy of the search space (Fig. 10b) is applied in order to identify the global optimum with

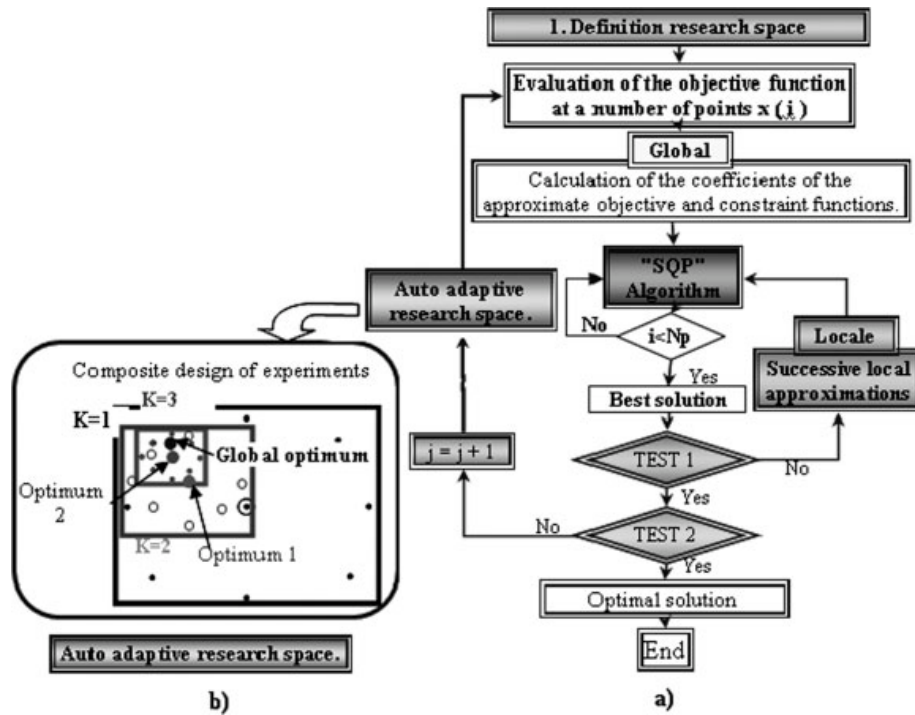


FIG. 10. The flowchart of the adopted optimization strategy.

lower cost. For this, during the progression of the procedure, the region of interest moves and zooms on each optimum. The goal is to reuse the interpolation points of the zoomed area and to enrich them with new interpolation points obtained by the new design of experiment. The iterative procedure stops when the successive optima are superposed with a tolerance $\varepsilon = 10^{-3}$ (Test no. 2).

EXAMPLE OF DIE DESIGN PROBLEMS

The optimization result relates to the improvement of the coat-hanger melt distributor geometry in order to ensure a homogeneous exit velocity distribution for a range of materials and for multiple operating conditions.

For the original design, we noted both numerically and experimentally, for two different materials in which the exit velocity is about 10% above average at the die entrance and about 20% below average at die exit.

The optimization example was carried out for LDPE Lupolen 1812D and with a flow rate of 132 kg/h. By symmetry, only one half die is modeled. To show the improvement of the exit velocity distribution compared with the initial design, we deferred on the convergence story the value of the objective function corresponding to the initial die geometry (a flat manifold of constant width $W_0 = 50$). The pressure obtained in the initial die geometry is 13.74 MPa. The constraint on the pressure was imposed so that the pressure in the optimal coat-hanger melt distributor does not exceed $P_0^e = 14$ MPa. The

TABLE 4. Summary of the results.

| Die design | Initial | Optimal |
|---|---------|-------------|
| CPU time | | 12 h 30 min |
| N simulations | — | 19 |
| N iterations | 0 | 2 |
| Total relative deviation E | 8.76 % | 0.81% |
| Objective function f | 1 | 0.09 |
| Improvement of the velocity distribution | — | 91% |
| Constraint function | 0.98 | 0.99 |
| Global relative deviation of the average velocities E_g^s | 52.23 | 2.68 |
| Improvement of the average velocity distribution | — | 95% |
| Variable W (mm) | 50 | 18.5 |
| Variable H (mm) | 5.51 | 5.5 |

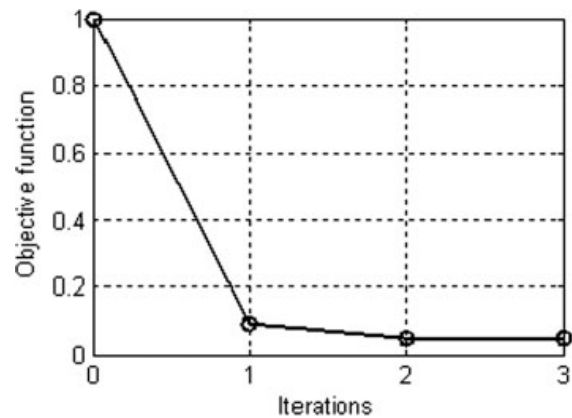


FIG. 11. Convergence history of the objective function.

TABLE 5. Relative velocity deviations (experimental data and numerical calculations).

| Data | 1 | | | 2 | | |
|------------------------------------|---------------|------------|------------|-------------|------------|------------|
| | Lupolen 1812D | | | LDPE 22H760 | | |
| | Initial | | Optimal | Initial | | Optimal |
| | Exp (%) | Calcul (%) | Calcul (%) | Exp (%) | Calcul (%) | Calcul (%) |
| E_1^s | 9.76 | 10.12 | 0.94 | 9.89 | 7.8 | 0.87 |
| E_2^s | 9.45 | 10.1 | 0.22 | 8.91 | 6.82 | 0.23 |
| E_3^s | 7.09 | 5.89 | 0.11 | 6.16 | 4.18 | 0.13 |
| E_4^s | 4.8 | 5.01 | 0.18 | 4.85 | 4.02 | 0.1 |
| E_5^s | 21.5 | 21.11 | 1.23 | 20.12 | 14.79 | 1 |
| Global relative deviations E_g^s | 52.58 | 52.23 | 2.68 | 49.93 | 37.61 | 2.34 |

results of optimization are carried out on a machine Pentium D, 3.4 GHz, 3.0 Go RAM.

Table 4 presents a summary of the results obtained with the initial and optimal die design. The total relative deviation obtained with the optimal die design is very weak of about 0.81%, which is equivalent to an improvement of about 91% compared with the reference design. The partial average exit velocity in the various sections is improved of about 95% compared with experimental measurements. We notes that the variable H did not change. On the other hand, the width W of the manifold is significantly reduced to a value of 18.5 mm at the manifold exit.

The convergence history during the optimization run is presented in Fig. 11. The optimal solution is obtained starting from the second iteration. The objective function is then reduced by 91%. The optimization strategy clearly showed its capacity to obtain an optimal solution with a very fast convergence.

Table 5 indicates the relative velocity deviations before and after optimization for two polymers of different rheological behaviors. We noted on Figs. 12 and 13 that, after optimization, the relative average velocities deviation for each section decreased considerably. This implies a better distribution on the optimal die for the two materials considered.

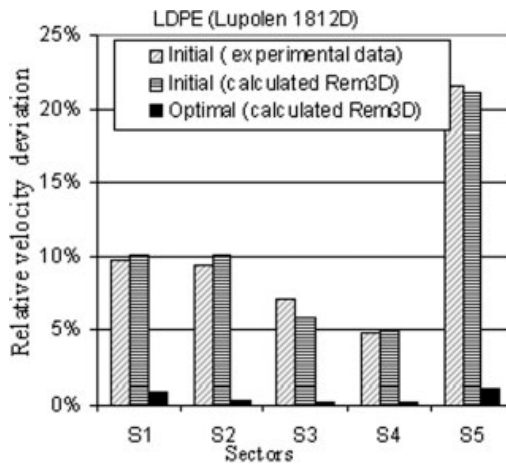


FIG. 12. Relative deviation of the average velocities in the different sectors (Lupolen 1812D).

We note in Fig. 14 that the optimized die design is independent of polymer viscosity, and a uniform velocity distribution is obtained for two materials with different rheologies. The pressure did not exceed the imposed initial pressure $P_0^s = 14$ MPa, and thus the constraint on the pressure level is respected. The pressure is higher in the case of Lupolen 1812D and it is weaker for the 22H760.

This optimization problem was formulated in way to find the best velocity distribution at the die exit while avoiding the increase of pressure compared with the pressure obtained in the initial die. If the second criterion (pressure drop in the die) is introduced like an objective function the result must be different and the optimization problem should be formulated to minimize the pressure drop in the die such that the exit velocity distribution (constraint function) must be uniform. The constraint function (g) is the computed exit velocity variation. A zero value of g indicates that the computed exit velocity equals the prescribed exit velocity over the entire width of the exit, i.e., the exit velocity is everywhere uniform. We can include a small tolerance ε on the exit velocity variation to avoid the numerical perturbations.

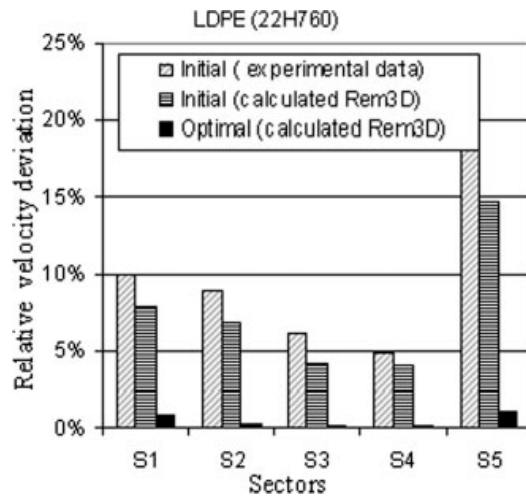


FIG. 13. Relative deviation of the average velocities in the different sectors (LDPE 22H760).

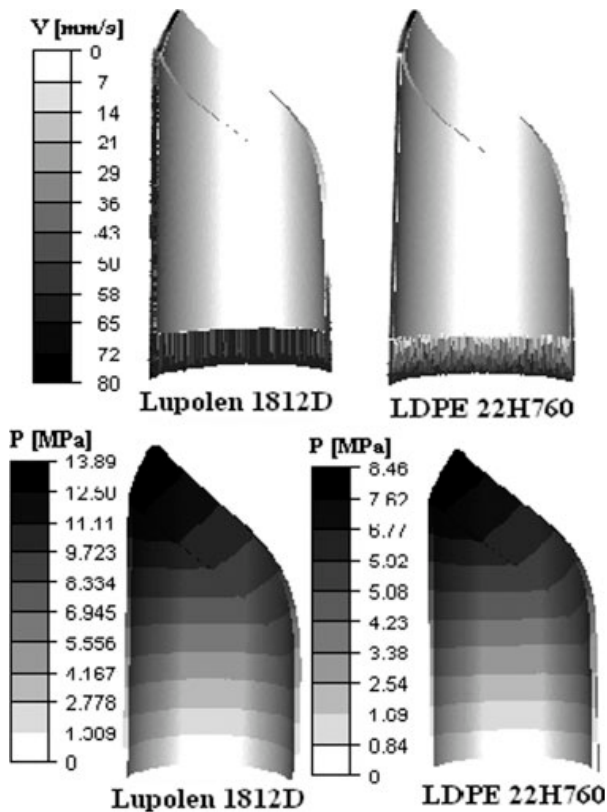


FIG. 14. Pressures and exit velocity distribution in optimal die design.

CONCLUSIONS

In this article, application of an optimization method for coat-hanger melt flow distributors is presented. The optimization method is based on a Surface Response Method and has a very fast convergence, which is an advantage when time-consuming flow analysis calculations are involved.

The method was applied to determine an optimal coat-hanger melt distributor starting from an existing design, for which experimental melt flow distribution performance was available. These experimental results were first used to validate the melt flow analysis calculation.

The optimized melt flow distributor showed an excellent distribution for materials with different rheological behaviors.

The numerical optimization algorithm presented in this work shows its suitability and robustness as a tool for extrusion die design. It proves its capability of predicting optimal die geometry with uniform velocity distribution for a range of polymers, at satisfactory computing times

for 3D Finite Element flow analysis. Future research will involve experimental verification of the optimization of complex helicoidally dies.

ACKNOWLEDGMENTS

The support of Maillefer SA is gratefully acknowledged.

REFERENCES

1. C. Chen, P. Jen, and F.S. Lai, *Polym. Eng. Sci.*, **37**, 188 (1997).
2. Y. Wang, *Polym. Eng. Sci.*, **31**, 204 (1991).
3. D.C. Montgomery, *Design and Analysis of Experiments*, John Wiley & Sons, New Jersey (2005).
4. D.E. Smith, D.A. Tortorelli, and C.L. Tucker, *Comput. Methods Appl. Mech. Eng.*, **167**, 283 (1998).
5. D.E. Smith, D.A. Tortorelli, and C.L. Tucker, *Comput. Methods Appl. Mech. Eng.*, **167**, 303 (1998).
6. Y. Sun and M. Gupta, "Optimization of a Flat Die Geometry," *SPE ANTEC Tech. Papers*, Chicago, IL, USA, May 16–20 (2004).
7. O.S. Carneiro, J.M. Nóbrega, F.T. Pinho, and P.J. Oliveira, "Automatic Balancing of Profile Extrusion Dies: Experimental Assessment," in *SPE ANTEC Tech. Papers*, Chicago, IL, USA, May 16–20 (2004).
8. W. Michaeli and S. Kaul, *J. Polym. Eng.*, **24**, 136 (2004).
9. L.G. Reifschneider, "Automated Sheet Die Design," in *SPE ANTEC Tech. Papers*, San Francisco, CA, USA, May 5–9 (2002).
10. D.E. Smith, "An Optimisation-based Approach to Compute Sheeting Die Designs for Multiple Operating Conditions," in *SPE ANTEC Tech. Papers*, Nashville, TN, USA, May 4–8 (2003).
11. H.H. Winter and H.G. Fritz, *Polym. Eng. Sci.*, **26**, 543 (1986).
12. D. Schläfli, *Int. Polym. Process.*, **10**, 195 (1995).
13. L. Silva, "Viscoelastic Compressible Flow and Applications in 3D Injection Molding Simulation," *Thèse de Doctorat, CEMEF* (2004).
14. R.H. Myers and D.C. Montgomery, *Response Surface Methodology, Process and Product Optimization Using Designed Experiments, 2nd ed.*, Wiley Interscience, New York (2002).
15. N. Lebaal, S. Puissant, and F.M. Schmidt, *J. Mater. Process. Technol.*, **34**, 1524 (2005).
16. I. Kaymaz, *Struct. Saf.*, **27**, 133 (2005).
17. N. Lebaal, S. Puissant, and F.M. Schmidt, "Optimizations of Coat-hanger Die, Using Constraint Optimization Algorithm and Taguchi Method," in *NUMIFORM '07, AIP Conference Proceedings* 908, 537 (2007).